Earth and Planetary Science Letters 551 (2020) 116587

Contents lists available at ScienceDirect

Earth and Planetary Science Letters

www.elsevier.com/locate/epsl

Volcanic ash ice-nucleating activity can be enhanced or depressed by ash-gas interaction in the eruption plume

Elena C. Maters [a,b,*], Corrado Cimarelli [c], Ana S. Casas [c], Donald B. Dingwell [c], Benjamin J. Murray [a]

[a] School of Earth and Environment, University of Leeds, Leeds LS2 9JT, United Kingdom
[b] Department of Chemistry, University of Cambridge, Cambridge CB2 1EW, United Kingdom
[c] Department of Earth and Environmental Sciences, Ludwig-Maximilians-Universität München, 80333 Munich, Germany

ARTICLE INFO

Article history:
Received 27 June 2020
Received in revised form 12 September 2020
Accepted 14 September 2020
Available online 23 September 2020
Editor: A. Rust

Dataset link: https://doi.org/10.5518/890

Keywords:
volcanic ash
ice nucleation
eruption plume
heterogeneous

ABSTRACT

Volcanic ash can trigger ice nucleation when immersed in supercooled water. This will impact several processes (e.g., electrification, aggregation, precipitation) in the eruption plume and cloud and in the wider atmosphere upon ash dispersal. Previous studies show that ash bulk properties, reflecting the chemistry and phase state of the source magma, likely contribute to the ice-nucleating activity (INA) of ash. However, it remains unexplored how interaction with magmatic gases in the hot eruption plume, which inevitably leads to altered ash surface properties, affects the ash INA. Here we demonstrate that the INA of tephra is raised by exposure to $H_2O_{(g)}$ mixed with $SO_{2(g)}$ at both 800 and 400 °C, but is substantially reduced by exposure to $H_2O_{(g)}$ alone or mixed with $HCl_{(g)}$ at the same temperatures. In contrast, the INA of K-feldspar and quartz is reduced by all three eruption plume processing treatments. The decrease in INA of all silicates after heating with $H_2O_{(g)}$ might relate to a loss of ice-active sites by surface dehydroxylation and/or oxidation. In the presence of $HCl_{(g)}$ or $SO_{2(g)}$, respectively, metal chloride or sulphate salts form on the tephra surfaces only. While NaCl and $CaCl_2$ seem to have no effect on the tephra INA, $CaSO_4$ is inferred to create ice-active sites, potentially through a particular combination of surface chemistry and topography. Overall, our findings suggest a complex interplay of bulk mineralogy and surface alteration in influencing ice nucleation by volcanic ash, and highlight the general sensitivity (enhancement or depression) of ash INA to interaction with magmatic gases in the eruption plume.

1. Introduction

Explosive volcanic eruptions generate mixed glassy and crystalline silicate ash that can serve as ice-nucleating particles (INPs). In the vertical eruption plume and the laterally dispersed eruption cloud, the freezing of supercooled water may impact a range of processes including plume/cloud electrification, gas scavenging, and ash aggregation (Van Eaton et al., 2015; Prata et al., 2020). In the wider atmosphere, ice formation on airborne ash may modify the properties and lifetime of clouds, thereby affecting precipitation and the Earth's radiation balance (Seifert et al., 2011). Volcanic activity worldwide produces a recurrent flux of ash to the atmosphere (176-256 Tg a^{-1}) (Durant et al., 2010), while sporadic large eruptions release substantial quantities of ash at one time (e.g., ~500 Tg on 18 May 1980 from Mt. St. Helens volcano, USA) (Nathenson, 2017), potentially boosting local to regional INP populations (Seifert et al., 2011; Hobbs et al., 1971).

The ability of ash to nucleate ice (its ice-nucleating activity; INA) when immersed in supercooled water (i.e. in the immersion mode) is influenced by various bulk properties. For example, broad correlations have been observed between the INA and the chemical composition of a range of milled ash samples; with INA increasing with K_2O content and decreasing with MnO, TiO_2, FeO/Fe_2O_3, MgO, and/or CaO contents (Genareau et al., 2018; Maters et al., 2019). These trends are thought to reflect an indirect influence on INA of the source magma composition, which dictates the types of crystalline phases likely to end up in the erupted ash and contribute to INA (Maters et al., 2019). Indeed, several studies highlight the role of mineralogy in explaining variation in INA by ash samples from different volcanoes and/or eruptions, with alkali (here 'K-', indicating K-rich) feldspars, plagioclase (here 'Na/Ca-') feldspars, pyroxenes, and potentially quartz inferred to impart a high INA to ash (Maters et al., 2019; Schill et al., 2015; Jahn et al., 2019). However, ice nucleation is an interfacial process and the

* Corresponding author.
E-mail address: ecm63@cam.ac.uk (E.C. Maters).

https://doi.org/10.1016/j.epsl.2020.116587

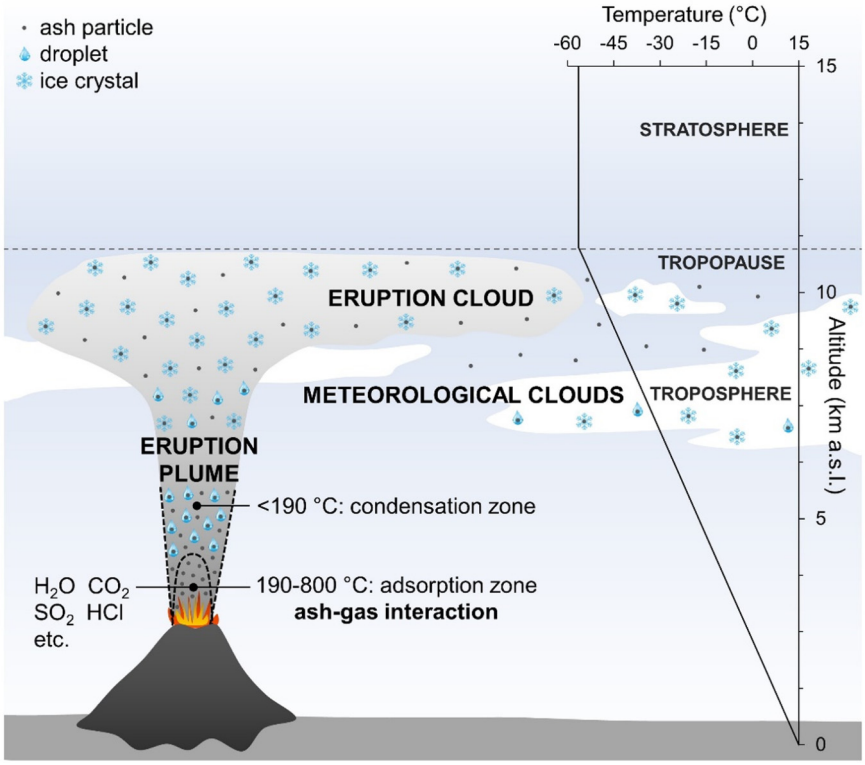

Fig. 1. Schematic of the eruption plume and cloud, meteorological clouds, and altitude-temperature profile of the international standard atmosphere (ISA). Note that the adsorption and condensation zones in the eruption plume (Óskarsson, 1980) are not shown to scale with respect to the ISA profile; the altitudes at which they occur depend on factors such as the volcano summit elevation, eruption magnitude, and air entrainment rate. The hot core of the plume, where ash-gas interaction takes place, is the context of 'eruption plume processing' in this study.

surface properties of ash differ from the bulk properties, due in part to interactions with magmatic gases including $H_2O_{(g)}$, $SO_{2(g)}$, $HCl_{(g)}$ and $HF_{(g)}$ at high temperatures (~200-800 °C) in the eruption plume (Óskarsson, 1980; Delmelle et al., 2007). This 'eruption plume processing' emplaces surficial metal sulphate and halide salts and modifies the surface chemical reactivity of ash (Óskarsson, 1980; Delmelle et al., 2007; Maters et al., 2016), but its influence on the INA of ash in particular is not known (Fig. 1).

Based on field measurements showing no increase in background INP concentrations following several volcanic eruptions, it has been suggested that exposure to magmatic $SO_{2(g)}$ deactivates the INA of ash particles (Langer et al., 1974; Schnell et al., 1982). Numerous experimental studies on mineral dusts have investigated the effects of gaseous and aqueous acids on INA. Treatment of montmorillonite with $SO_{2(g)}$ had no impact on its ability to nucleate ice from water in the vapour phase (i.e. in the deposition mode) (Salam et al., 2008), while exposure of Arizona test dust (ATD) to HNO_3 vapour reduced, promoted, or had no effect on INA below, near, or above water saturation, respectively (Sullivan et al., 2010a). Treatment of kaolinite, illite, K-feldspar and ATD with H_2SO_4 vapour and heat (70-250 °C) reduced deposition and/or immersion mode INA (Sullivan et al., 2010b; Wex et al., 2014; Augustin-Bauditz et al., 2014). Additionally, contact with dilute alkali salt solutions (K_2SO_4, Na_2SO_4, KCl, NaCl; 10^{-4} to 1 M) has been shown to decrease the INA of some silicates including K- and Na/Ca-feldspars compared to when they are immersed in pure water (Whale et al., 2018; Kumar et al., 2018, 2019a). This has been proposed to reflect a suppressed exchange, in the presence of dissolved K^+ and Na^+, of alkali cations from the silicate surfaces with H^+/H_3O^+ from solution, a process that may be important in ice nucleation by these materials (Kumar et al., 2018, 2019a). Further, dissolved SO_4^{2-} may form complexes with Al and thereby promote Al dissolution and -OH group removal from the silicates, potentially blocking or destroying surface sites at which ice nucleation occurs (ice-active sites) (Kumar et al., 2018, 2019a). Collectively, these findings suggest that in-plume exposure to acidic gases and emplacement of soluble metal sulphate and halide salts might depress the INA of volcanic ash. However, the conditions simulated in various 'atmospheric processing' studies on dust differ substantially from the extreme thermal and chemical conditions to which ash is exposed in an eruption plume, calling for dedicated investigation of the effects of high temperature ash-gas interaction on the INA of ash.

Heating of silicates (e.g., silica and soda-lime-silica glass, Na/Ca-feldspar, quartz, kaolinite) >400 °C can result in condensation of adjacent Si-OH groups to form Si-O-Si bridges, producing a more hydrophobic and compact silica-like surface (Schaeffer et al., 1986; Temuujin et al., 1999; D'Souza and Pantano, 2002). This removal of surface -OH groups (also known as dehydroxylation) can be enhanced by the presence of H_2O vapour (Temuujin et al., 1999) and can become irreversible as the heating temperature is raised >400 °C (D'Souza and Pantano, 2002). Powdered K-feldspar can also be converted to an amorphous state when 'highly heated,' although no temperature is stated in the patent describing this effect (Swayze, 1907). Additionally, Fe-containing silicates undergo oxidation of Fe^{2+} to Fe^{3+} at high temperatures (550-1100 °C), accompanied by an outward diffusion of divalent cations (e.g., Mg^{2+}, Fe^{2+}, Ca^{2+}) (Wu et al., 1988; Cooper et al., 1996). Oxidation of Fe^{2+} likely reduces the mobility of alkali cations such as Na^+ and K^+, as these cations may become fixed in a charge-compensating role to accommodate newly-formed Fe^{3+} in the silicate network (Cooper et al., 1996; Pelte et al., 2000).

Exposure of silicates (e.g., multi-oxide silicate glasses, Na/Ca-feldspar, pyroxene, Kilauea basalt, Mono Craters obsidian) to $SO_{2(g)}$ and $HCl_{(g)}$ at high temperatures can lead to the formation of metal sulphate and chloride salts as reaction products (Delmelle et al., 2018; King et al., 2018; Renggli et al., 2019). For example,

Table 1
Details of the silicate materials used in this study.

Material	Code	Source	Mineralogy[d] (wt.%)						SSA_{BET} ($m^2 g^{-1}$)[e]	
			Alk. feld.	Plag. feld.	Pyrox.	Quartz	Fe(-Ti) oxide	Glass	Treatment	
Tungurahua tephra[a]	TUN tephra	Tungurahua volcano, Ecuador, February 2014 eruption	-	43	11	-	m.c.	46	none	1.4
									H_2O	1.2
									H_2O-SO_2	0.9
									H_2O-HCl	1.1
Astroni tephra[a]	AST tephra	Astroni volcano, Italy, 3.8-4.4 ka eruption	19	7	2	-	m.c.	72	none	3.7
									H_2O	2.5
									H_2O-SO_2	1.5
									H_2O-HCl	1.8
Etna tephra[a]	ETN tephra	Etna volcano, Italy, July 2014 eruption	-	44	22	-	m.c.	34	none	1.7
									H_2O	1.2
									H_2O-SO_2	0.9
									H_2O-HCl	1.2
Alkali feldspar[b]	FELD	BSC 376 microcline, Bureau of Analysed Samples Ltd	80.1	16	-	3.9	-	-	none	1.9
									H_2O	1.8
									H_2O-SO_2	1.5
									H_2O-HCl	1.7
Smoky quartz[c]	QRTZ	Pikes Peak mountain, United States of America	-	1.6	-	98.3	0.1	-	none	1.4
									H_2O	1.2
									H_2O-SO_2	1.2
									H_2O-HCl	1.2

Mineralogy reported in [a]Maters et al. (2019), [b]Atkinson et al. (2013), [c]Harrison et al. (2019).
[d]Alk. feld. = K-feldspar, Plag. feld. = Na/Ca-feldspar, Pyrox. = pyroxene, Glass = amorphous (non-crystalline), m.c. = minor component below ~2 wt.% quantification limit by X-ray diffraction in that study.
[e]Uncertainty is in the range of 0.5-1.2%.

$SO_{2(g)}$ interacts with soda-lime-silica glass and volcanic glasses at 400 to 800 °C to produce primarily Na_2SO_4 and $CaSO_4$, respectively (Douglas and Isard, 1949; Ayris et al., 2013; Casas et al., 2019). These sulphate compounds are argued to reflect the reaction of adsorbed SO_2 with alkali or alkaline earth cations (e.g., Na^+, K^+, Ca^{2+}, Mg^{2+}) at the silicate surface. Further, $HCl_{(g)}$ interacts with soda-lime-silica, mixed-alkali borosilicate, and volcanic tephrite and phonolite glasses at 300 to 700 °C to produce primarily NaCl (Schaeffer et al., 1986; Sung et al., 2009; Ayris et al., 2014). This is proposed to involve the reaction of Cl^- from adsorbed HCl with Na^+ at the glass surface. Differences in cation diffusivities, which vary as a complex function of factors such as silicate composition and heating temperature, are thought to dictate which particular salts form Renggli et al. (2019). Cation extraction by reaction with $SO_{2(g)}$ or $HCl_{(g)}$ at high temperatures generates a compacted, cation-depleted and silica-enriched surface beneath the salts (Renggli et al., 2019; Ayris et al., 2014; Li et al., 2010). This process of 'dealkalisation' is often exploited in the glass industry to enhance surface resistance to chemical weathering, for instance by blocking further diffusive exchange of cations (Schaeffer et al., 1986).

While these studies shed light on how various high temperature gas-solid interactions might alter the surface properties of volcanic ash, the influence of such interactions on the ability of ash to nucleate ice has yet to be explored. Here we expose three compositionally distinct tephra samples, a K-feldspar sample, and a quartz sample to gas mixtures comprising $H_2O_{(g)}$, $SO_{2(g)}$, and/or $HCl_{(g)}$ under a heating sequence of 800 and then 400 °C, and assess the INA of the non-treated and treated samples in the immersion mode using cold stage droplet assays. By uniquely combining in-plume gas-solid interaction simulations with ice nucleation measurements of various silicate materials, this experimental study contributes new insights on the potential impacts of eruption plume processing on the INA of volcanic ash before it disperses in the eruption cloud and wider atmosphere.

2. Materials and methods

2.1. Silicate samples

Three volcanic tephra samples (from eruptions of Tungurahua, Astroni and Etna volcanoes), a K-feldspar (BCS 376 microcline), and a crystalline silica (smoky quartz) were studied (Table 1). These silicate materials have been characterised in terms of chemical and/or mineralogical composition as well as INA in previous studies (Maters et al., 2019; Atkinson et al., 2013; Harrison et al., 2016, 2019). As in those studies, the materials here were crushed to fine powders in a ball mill using a zirconia ceramic ball and vial, but were not otherwise subjected to physical or chemical alteration, prior to eruption plume processing treatments (see section 2.2). Milling of the materials exposed fresh surfaces to test the influence of gas-solid interaction on INA under controlled conditions in the laboratory. Any pre-existing salts on the tephra would have remained in the powders but only on a small fraction of surfaces following milling. The specific surface area (SSA_{BET}) of the non-treated and treated samples was obtained, after overnight degassing, from a 10-point N_2 adsorption isotherm at -196 °C based on the Brunauer, Emmet, and Teller model.

2.2. Eruption plume processing treatments

An Advanced Gas-Ash Reactor (AGAR), capable of simulating thermal and chemical properties found within the hot core of a volcanic eruption plume (Ayris et al., 2015), was used to subject the five silicate materials to high temperature gas-solid interaction. Specifically, sub-samples of these materials were heated under three distinct gas compositions in the AGAR, and the influence of thermochemical treatment on the materials' INA was subsequently assessed by ice nucleation experiments (see section 2.3). Note that the treatments are not designed to reproduce the actual experience of ash particles in an eruption plume - being unable

to replicate the precise conditions and timescales of in-plume processing (Ayris et al., 2015) - but rather to shed light on factors that can affect the INA of ash.

Gas compositions of pure $H_2O_{(g)}$ (H_2O), $H_2O_{(g)}$ mixed with $SO_{2(g)}$ ($H_2O - SO_2$), and $H_2O_{(g)}$ mixed with $HCl_{(g)}$ ($H_2O - HCl$) were chosen for this investigation, as these species are among the main gases co-erupted with volcanic ash. Sequential heating at 800 and then 400 °C was applied to cover the in-plume temperature ranges in which $SO_{2(g)}$ and $HCl_{(g)}$ have been reported to react most efficiently with an array of silicate glasses and minerals (King et al., 2018; Ayris et al., 2013, 2014). Gas delivery to the AGAR consisted of a 50 sccm flow of $Ar_{(g)}$ containing H_2O (0.4 ml min^{-1} inlet flow) aerosolised by a quartz nebuliser, and a 100 sccm flow of $Ar_{(g)}$ on its own or mixed (75:25 sccm) with $SO_{2(g)}$ (1 mol.% in $Ar_{(g)}$) or $HCl_{(g)}$ (1 mol.% in $Ar_{(g)}$). Excluding the contribution of the inert $Ar_{(g)}$ carrier, the mixed gas flows produced compositions of 62 to 100 mol.% $H_2O_{(g)}$ and 1 mol.% $SO_{2(g)}$ or 1 mol.% $HCl_{(g)}$, consistent with the ranges of measured near-vent volcanic gas concentrations (Ayris et al., 2015).

Each sub-sample (~2 g) of volcanic tephra, K-feldspar, or quartz was loaded into the sample bulb, inserted horizontally into the working tube of the AGAR's three-stage furnace, and rotated continuously (7 rpm) to overturn the powder during exposure to heat and gases. A fast insertion protocol was applied in all experiments. This consisted of sliding the sample bulb into the furnace region at ~800 °C; turning on the nebuliser, gas flows, and rotation for 600 s; then sliding the sample bulb into the furnace region at ~400 °C for 600 s; and finally turning off the nebuliser, gas flows, and rotation and removing the sample bulb from the reactor. The treated sample was allowed to cool to room temperature in air and then stored in a sealed vessel until further experiments and analyses (e.g., see sections 2.3 and 2.4).

2.3. Ice nucleation experiments

A microlitre Nucleation by Immersed Particles Instrument (μL-NIPI) was used to assess the INA of the non-treated and treated samples. This instrument has been detailed by Whale et al. (2015) and used in various studies of ice nucleation by silicate materials (Maters et al., 2019; Atkinson et al., 2013; Harrison et al., 2016, 2019). Briefly, a 1 wt.% suspension of sub-sample in Milli-Q water (18.2 MΩ·cm) was shaken for a few minutes by a vortex mixer, and then pipetted in an array of 1 μL droplets (30-45) onto a silanised glass cover slip on a temperature-controlled stage (Grant-Asymptote EF600 Stirling Cryocooler). The stage was cooled at a rate of -1 °C min^{-1} below 0 °C until all droplets were frozen. A dry $N_{2(g)}$ flow (~0.2 L min^{-1}) was applied over the droplets to prevent condensation and frost accumulation on the cover slip and, thus, to avoid frozen droplets affecting neighbouring liquid droplets. A digital camera was used to monitor the droplets during the experiment and to determine the fraction of droplets frozen as a function of temperature $f_{ice}(T)$, used to calculate the ice nucleation active site density $n_s(T)$, i.e., the number of ice-active sites per unit surface area of a solid sample on cooling from 0 °C down to temperature (T) (Connolly et al., 2009):

$$f_{ice}(T) = \frac{n_{ice}(T)}{n} = 1 - \exp(-n_s(T)\,A),$$

where $n_{ice}(T)$ is the cumulative number of droplets frozen at temperature (T), n is the total number of droplets in the experiment, and A is the total surface area of the solid sample per droplet. The parameter $n_s(T)$ allows us to empirically define the INA of a range of materials, even though the fundamental nature of ice-active sites remains unclear. The uncertainty in $n_s(T)$ was calculated using Monte Carlo simulations of possible ice-active site distributions across droplets, and incorporating Poisson counting statistics to account for sampling errors, as in Harrison et al. (2019). Experiments were conducted at least in triplicate for each sample. Additionally, ice nucleation of the background water due to impurities in the water or effects of the cover slip was assessed by baseline droplet freezing measurements of water containing no added sample. The $n_s(T)$ data for each sample experiment were corrected to account for the potential background contribution to ice nucleation as in Vali (2019).

2.4. Water leachate analyses

Water leachate analysis can contribute to identifying and quantifying the soluble surface species emplaced during gas-solid interactions, including those occurring within the hot core of a volcanic eruption plume or within a high temperature reactor such as the AGAR (Delmelle et al., 2007; Ayris et al., 2013; Casas et al., 2019; Ayris et al., 2014; Witham et al., 2005). Specifically, leachates of the non-treated and treated samples were acquired here to gain insight on potential soluble surface products arising from the different eruption plume processing treatments (see section 2.2), and to assess the concentrations of dissolved elements and ions likely to be present in the 1 wt.% suspensions of sample in water utilised for ice nucleation experiments (see section 2.3).

Sub-samples of the non-treated and treated materials were rinsed in Milli-Q water at a 1 wt.% concentration and under constant gentle rotation for 30 min, i.e., reflecting a typical duration of an ice nucleation experiment. The leachates were then filtered through 0.2 μm cellulose acetate membrane filters and divided into three aliquots; one directly for measurement of SO_4^{2-} and Cl^- concentrations by ion chromatography (Thermo Scientific Dionex ICS-5000$^+$), another acidified to 1.5 vol.% HNO_3 for measurement of Na, K, Ca, Mg, and Fe concentrations by inductively coupled plasma - optical emission spectrometry (Thermo Scientific iCAP 7400 Radial ICP-OES), and the remainder stored in a sealed vessel under refrigeration (~4 °C). Quantification limits were 0.2 μM for SO_4^{2-}, 0.8 μM for Cl^-, 7 μM for Na, 3 μM for K, 0.3 μM for Ca, 0.05 μM for Mg, and 0.1 μM for Fe. Additionally, water-rinsed solid sub-samples retained from the leachates by filtration were left to dry in air overnight (under weighing paper) and then stored in a sealed vessel. The leachates and the water-rinsed sub-samples of the treated tephra were used later to investigate the influence of soluble surface species on the INA of the tephra (see sections 4.2 and 4.3).

3. Results

3.1. Ice-nucleating activity

All high temperature gas-solid interactions were expected to deactivate the INA of the silicate materials based on the literature surveyed in the introduction. However, the behaviour of these materials following the eruption plume processing treatments varied considerably, with an enhancement in INA observed in some cases. Fig. 2 shows the $n_s(T)$ values of the non-treated and treated samples from replicate ice nucleation experiments. The difference in INA between the treated and non-treated samples is summarised in Fig. 3 (with the temperature at which $n_s \approx 5$ cm^{-2}, $T_{ns\approx5cm^{-2}}$, chosen as a single-number proxy for INA; Table S1 in the SI).

For all materials, the H_2O treatment decreased the INA relative to that of the non-treated sample ($T_{ns\approx5cm^{-2}}$ lowered by 1.7 ± 3.0 to 15.0 ± 1.8 °C), although this decrease is within the error for ETN tephra. Similarly, the $H_2O - HCl$ treatment decreased the INA relative to that of the non-treated sample ($T_{ns\approx5cm^{-2}}$ lowered by 4.0 ± 3.7 to 16.2 ± 1.9 °C), to the same extent as the decrease induced by the H_2O treatment (tephra and quartz) or more (K-feldspar). In

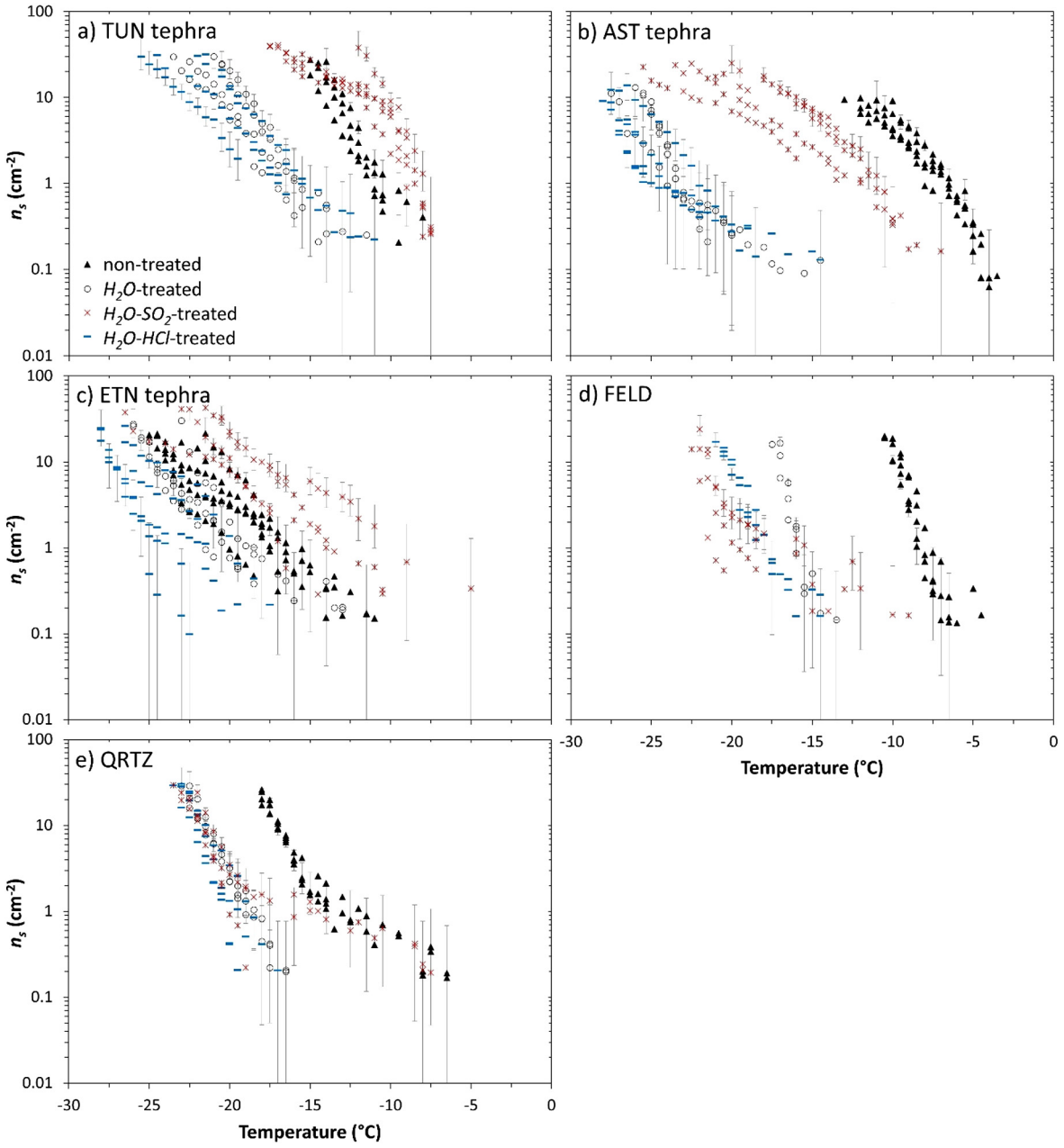

Fig. 2. Ice nucleation active site density (n_s) as a function of temperature for 1 wt.% suspensions of a) TUN tephra, b) AST tephra, c) ETN tephra, d) FELD, and e) QRTZ in water. Each plot shows replicates of the non-treated (black triangles), H_2O-treated (black unfilled circles), $H_2O - SO_2$-treated (red stars), and $H_2O - HCl$-treated (blue dashes) silicate samples. The uncertainty in n_s (T) is shown as error bars for a subset of experiments (one for each of the non-treated and treated samples) and omitted from replicates for clarity. Sample codes are listed in Table 1. (For interpretation of the colours in the figure(s), the reader is referred to the web version of this article.)

contrast, exposure of the materials to $H_2O - SO_2$ elicited remarkably different impacts on their ability to nucleate ice. Relative to the non-treated sample, TUN- and ETN tephra display an enhanced INA following $H_2O - SO_2$ treatment ($T_{ns\approx5cm^{-2}}$ raised by 2.8 ± 1.3 to 4.0 ± 3.8 °C), whereas AST tephra, K-feldspar and quartz show a depressed INA following $H_2O - SO_2$ treatment ($T_{ns\approx5cm^{-2}}$ lowered by 4.8 ± 0.5 to 12.3 ± 0.8 °C). In comparison to the reduction elicited by the H_2O and $H_2O - HCl$ treatments, the $H_2O - SO_2$ treatment raised the INA of all three tephra, reduced further the INA of the K-feldspar, and had no additional effect on the INA of the quartz.

Overall, while observations for the K-feldspar and quartz are consistent with our hypothesis of deactivation of ice nucleation by heat and/or acids, the increased INA of the tephra exposed to $H_2O_{(g)}$ mixed with $SO_{2(g)}$ at high temperatures is striking and is contrary to expectations.

3.2. Water leachate chemistry

The chemical composition of the water leachates, in terms of the elements and ions released per unit surface area of the silicate samples, is shown in Fig. 4. For all five silicates, the non-treated and H_2O-treated sample leachates contain variable amounts of Na, K, Ca, Mg, Fe, SO_4^{2-} and Cl^- in concentrations below ~5 µmol m^{-2} (Fig. 4a, b). For the non-treated tephra, some of these dissolved species may originate from small amounts of pre-existing salt compounds present in the milled powders. Similar quantities (<5 µmol m^{-2}) of elements and ions are seen in the leachates of the $H_2O - SO_2$– and $H_2O - HCl$–treated K-feldspar and quartz

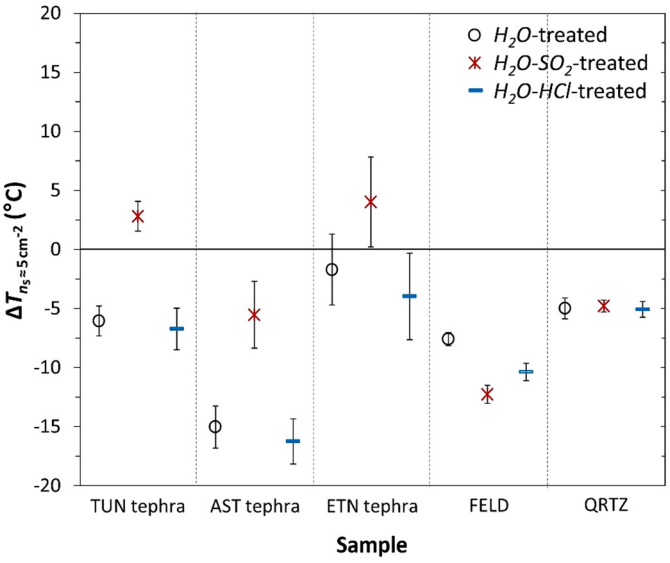

Fig. 3. Difference in INA ($\Delta T_{ns\approx5cm^{-2}}$) between the H_2O-treated (black unfilled circles), $H_2O - SO_2$-treated (red stars), or $H_2O - HCl$-treated (blue dashes) and the non-treated silicate samples. Values above or below the horizontal black line indicate that the INA of the treated samples is higher or lower, respectively, than the INA of the non-treated samples. The error bars reflect the ranges of values based on the standard deviations of mean $T_{ns\approx5cm^{-2}}$ values for the treated and non-treated samples from replicate ice nucleation experiments (Table S1). Sample codes are listed in Table 1.

(Fig. 4c, d), indicating no substantial difference in the amount of soluble material on these silicates irrespective of gas-solid interaction. Conversely, for the three tephra, considerably more soluble material is present after exposure to $SO_{2(g)}$ or $HCl_{(g)}$ in addition to $H_2O_{(g)}$ at high temperatures (Fig. 4c, d, note the difference in scale from Fig. 4a, b). Specifically, the $H_2O - SO_2$-treated tephra leachates are characterised by high concentrations of Na (42-175 µmol m^{-2}), Ca (150-209 µmol m^{-2}), Mg (25-90 µmol m^{-2}) and SO_4^{2-} (179-348 µmol m^{-2}), along with some K (18 and 22 µmol m^{-2}) in the case of AST- and ETN tephra (Fig. 4c). The $H_2O - HCl$-treated tephra leachates contain an abundance of Na (~4-130 µmol m^{-2}), Ca (13-17 µmol m^{-2}), Cl^- (~5-140 µmol m^{-2}), and SO_4^{2-} (~9-13 µmol m^{-2}; Fig. 4d). Sulphate in the $H_2O - HCl$-treated tephra leachates in concentrations above those measured in the non-treated tephra leachates might indicate some $SO_{2(g)}$ contamination in the gas lines during $H_2O - HCl$ experiments in the AGAR (Ayris et al., 2014).

4. Discussion

Based on previous studies on mineral dust, it was expected that the INA of the silicate materials here would be universally deactivated by eruption plume processing, but instead these materials exhibited highly variable responses to the three thermochemical treatments. These responses are grouped in the following discussion around trying to relate the observed changes in INA to the suspected modifications of the silicate surfaces induced by the different high temperature gas-solid interactions.

4.1. H_2O depresses the INA of the silicate materials

Exposure to H_2O reduced the INA of all five silicate materials (Fig. 2), however, the dissolved element and ion concentrations in the H_2O-treated sample leachates do not differ substantially from those in the non-treated sample leachates (Fig. 4a, b). This indicates that interaction between the materials and $H_2O_{(g)}$ at high temperatures did not lead to the formation of readily soluble compounds on their surfaces, and so the reduced INA is inferred to relate to some other chemical and/or physical change to the silicate surfaces during H_2O treatment.

Partial surface dehydroxylation of the H_2O-treated samples at temperatures >400 °C might explain the decrease in their INA relative to the non-treated samples. Specifically, surface -OH groups are thought to play an important role in heterogeneous ice nucleation as they can engage in hydrogen bonding with H_2O molecules to facilitate ice formation (Hu and Michaelides, 2007; Pedevilla et al., 2017). Hence, irreversible condensation of some surface Si-OH groups to Si-O-Si bridges during heat treatment likely reduced the abundance of ice-active sites on the silicate materials, since O atoms in Si-O-Si lack sufficient electronegativity for hydrogen bonding. Variation in the extent of INA reduction observed for the H_2O-treated samples (Fig. 3) probably reflects differences in individual properties of the silicates, such as the abundance and arrangement of -OH groups, which render their surfaces variably susceptible to the effects of high temperatures in the presence of $H_2O_{(g)}$.

Further, surface compaction (by dehydroxylation) of the H_2O-treated samples and/or oxidation of Fe^{2+} to Fe^{3+} (where present) might have inhibited the exchange of alkali cations such as Na^+ and K^+ with aqueous H^+/H_3O^+ on input of the samples to water during ice nucleation experiments. In other words, these processes might have hindered the surface protonation of immersed solid particles, which has been suggested to be a key step in ice nucleation by silicates bearing exchangeable cations (Kumar et al., 2018, 2019a).

In some cases, if exposure to high temperatures resulted in the formation of a silica-like surface on the H_2O-treated samples that is more amorphous (less crystalline) than the original surface (e.g., for K-feldspar) (Swayze, 1907), this might also have contributed to the reduction in INA observed after the H_2O treatment. Amorphous silicates have been shown, in general, to be less ice-active than crystalline silicates (Maters et al., 2019; Kumar et al., 2019b).

Ice nucleation on silicate materials is thought to be a site-specific phenomenon, i.e., nucleation occurs at specific sites on the solid surface (Holden et al., 2019). Therefore, the effects of eruption plume processing on INA presumably reflect changes to the properties of these specific sites, rather than changes to the bulk surface. It has been suggested that microscopic patches of high-energy faces, exposed at surface defects (e.g., edges, cracks) and containing a high density of -OH groups, give rise to effective sites for ice nucleation (Harrison et al., 2019; Pedevilla et al., 2017; Kiselev et al., 2017). These patches are typically unstable and tend to undergo thermochemical alteration more readily than the bulk surface (Holdren and Speyer, 1985). By analogy, dehydroxylation and/or oxidation during H_2O treatment might have occurred preferentially at high-energy sites on the silicate surfaces, potentially where elevated hydrogen bonding and/or protonation capabilities play a role in ice nucleation.

4.2. H_2O-HCl depresses the INA of tephra

As observed for H_2O, exposure to $H_2O - HCl$ reduced the ability of the silicate materials to nucleate ice (Fig. 2), with the depression in INA elicited by the $H_2O - HCl$ treatment either comparable to (for tephra and quartz) or greater than (for K-feldspar) the depression in INA elicited by the H_2O treatment alone (Fig. 3).

The three tephra display significantly higher concentrations of several dissolved elements and ions (Na, Ca, Cl^-, SO_4^{2-}) in the $H_2O - HCl$-treated sample leachates than in the non-treated sample leachates (Fig. 4a, d), suggesting that interaction with $H_2O_{(g)}$ and $HCl_{(g)}$ at high temperatures led to the emplacement of readily soluble compounds on the tephra surfaces. In particular, the relative molar abundances of various dissolved species, with Na:Cl^- ratios ranging from 0.7:1.0 to 0.9:1.0 and Ca:SO_4^{2-} ratios ranging

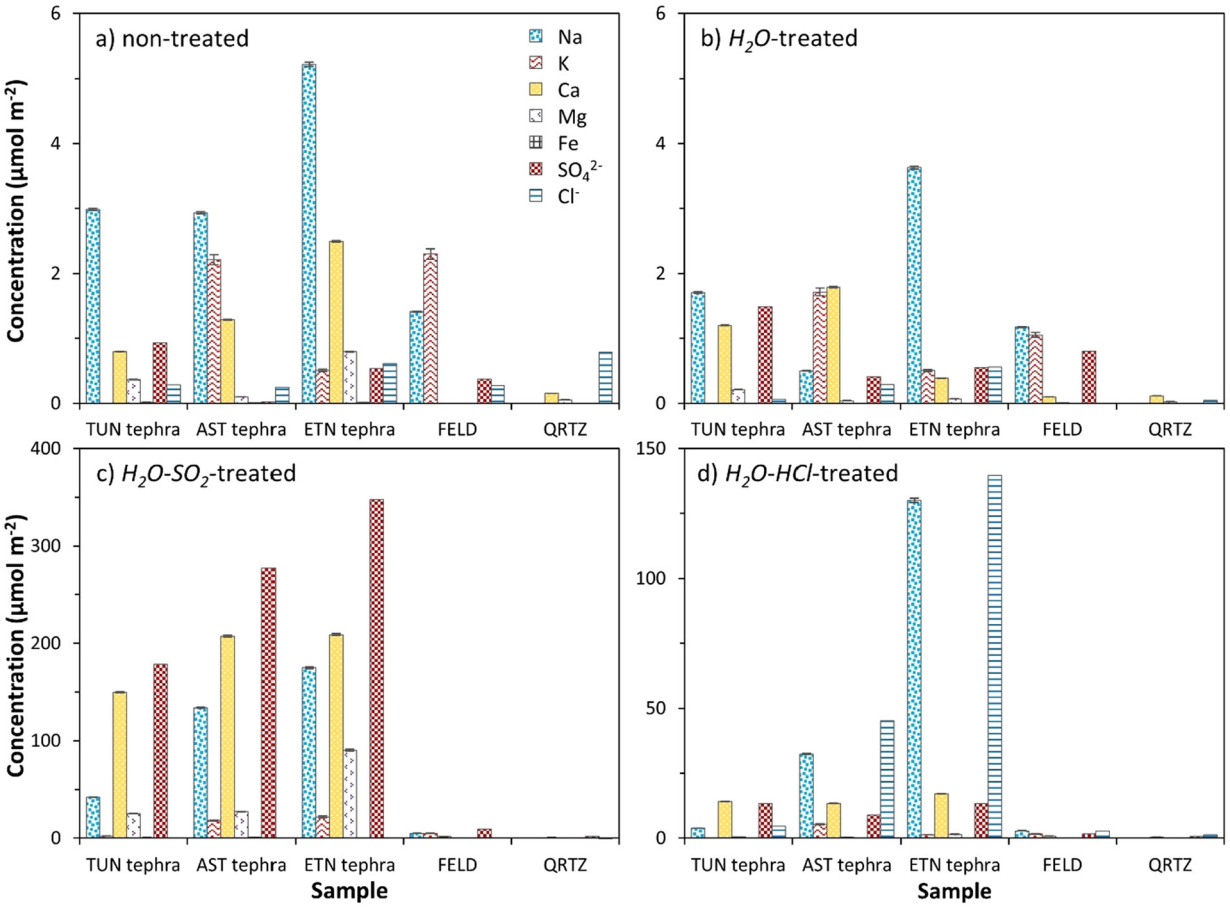

Fig. 4. Dissolved Na, K, Ca, Mg, Fe, SO_4^{2-}, and Cl^- concentrations per unit solid surface area in water leachates of the a) non-treated, b) H_2O-treated, c) $H_2O - SO_2$-treated, and d) $H_2O - HCl$-treated silicate samples. The samples were leached in water at 1 wt.% and under constant gentle rotation for 30 min, prior to filtration and analyses of the leachate. Sample codes are listed in Table 1.

from 1.1:1.0 to 1.5:1.0, may point to their presence in the form of NaCl, $CaSO_4$, and potentially $CaCl_2$ on the $H_2O - HCl$-treated tephra (Ayris et al., 2014). Despite reaction of the tephra material with $HCl_{(g)}$ to produce readily soluble surface salts (Fig. 4d), however, there appears to be no greater adverse effect of treatment with $HCl_{(g)}$ in addition to $H_2O_{(g)}$ on the INA of the tephra (Figs. 2, 3). Presumably, the $H_2O - HCl$-treated tephra surfaces underlying such salts, once immersed in water, exhibit similar ice-nucleating properties to the H_2O-treated tephra surfaces; with both sets likely featuring a more oxidised, compact and silica-rich layer with fewer sites for hydrogen bonding and/or ion exchange.

Dissolved alkali chlorides and sulphates have been shown to lower the INA of various silicates (Whale et al., 2018; Kumar et al., 2018, 2019a). Hence, one might have expected a solute-related suppression of INA following dissolution of metal chloride and sulphate salts from the $H_2O - HCl$-treated tephra in water (Fig. 4d) during ice nucleation experiments. To investigate whether the soluble salts produced by eruption plume processing could be responsible for modifying the volcanic tephra's ability to nucleate ice, supplementary experiments were carried out on TUN-, AST- and ETN tephra; measuring the INA of the non-treated tephra suspended in the $H_2O - HCl$-treated tephra leachates in addition to those suspended in Milli-Q water (Fig. 5). The similarity in INA of the non-treated tephra suspended in Na/Ca/Cl^-/SO_4^{2-}-rich leachate (10^{-2} to 10^{-1} M; Fig. 4d) and in pure water suggests that solute ions originating from metal chloride and sulphate salts are unlikely to explain the depressed INA of the $H_2O - HCl$-treated tephra. Moreover, the water-rinsed $H_2O - HCl$-treated tephra recovered after leaching and filtration (see section 2.4) also display a reduced INA relative to the non-treated tephra (Fig. 6). These tests show that the decreased ability of tephra exposed to $H_2O_{(g)}$ and $HCl_{(g)}$ at high temperatures to nucleate ice does not relate simply to its soluble surface salts, but rather to irreversible changes in the tephra surface underlying these salts.

4.3. H_2O-SO_2 enhances the INA of tephra

It is striking that the $H_2O - SO_2$-treated tephra displayed an enhanced INA relative to the non-treated and/or H_2O- and $H_2O - HCl$-treated tephra (Figs. 2, 3). From these observations, it is inferred that reaction of the tephra with $SO_{2(g)}$ altered these materials in such a way that either partially offsets or entirely overcomes the negative influence of exposure to $H_2O_{(g)}$ alone at high temperatures on their ability to nucleate ice (see section 4.1).

We first address the possibility that this reflects a positive influence of solute ions on INA following dissolution of metal sulphate salts from the $H_2O - SO_2$-treated tephra in water (Fig. 4c) during ice nucleation experiments. The three tephra display significantly higher concentrations of most dissolved elements and ions (Na, K, Ca, Mg, SO_4^{2-}) in the $H_2O - SO_2$-treated sample leachates than in the non-treated sample leachates (Fig. 4a, c), implying that interaction with $H_2O_{(g)}$ and $SO_{2(g)}$ at high temperatures resulted in the emplacement of readily soluble compounds on the tephra surfaces. Specifically, the relative molar abundances of various dissolved species, with (Na/2+K/2+Ca+Mg):SO_4^{2-} ratios of 1.1:1.0, may indicate their occurrence in the form of metal sulphate salts on the $H_2O - SO_2$-treated tephra. For illustration, surficial deposits rich in Ca and S, likely corresponding to anhydrite (anhydrous

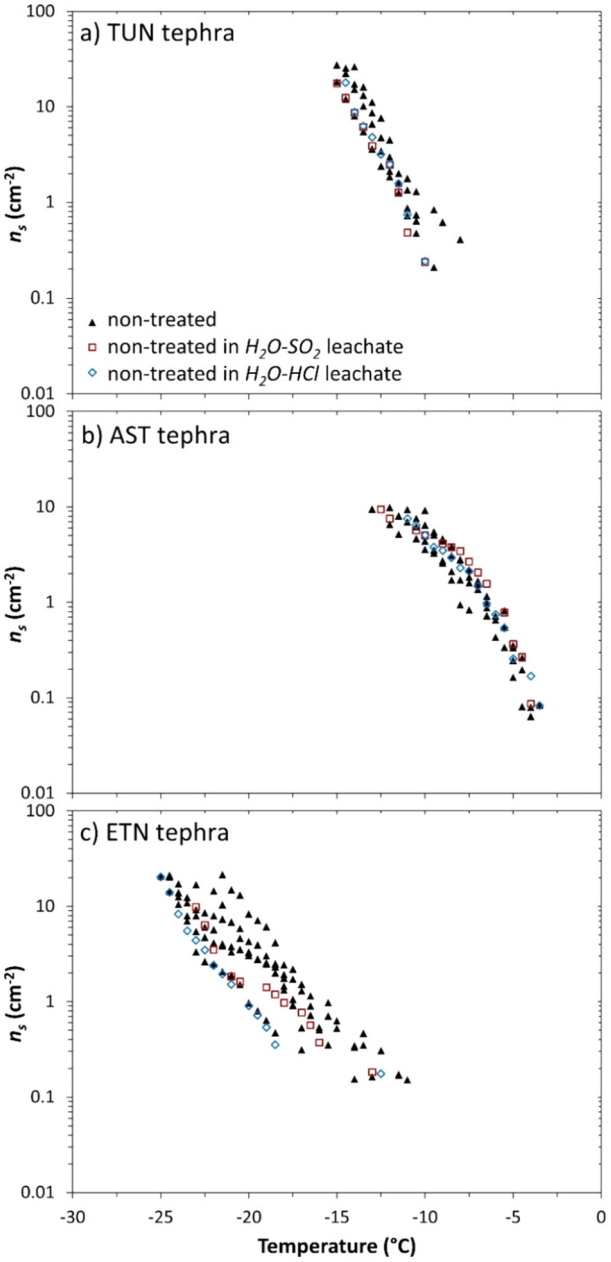

Fig. 5. The INA of the non-treated tephra samples in water versus in solute-rich leachate. Ice nucleation active site density (n_s) as a function of temperature for 1 wt.% suspensions of a) TUN tephra, b) AST tephra, and c) ETN tephra. These include replicates of the non-treated tephra samples in water (black triangles), in the $H_2O - SO_2$-treated tephra leachate (red unfilled squares), or in the $H_2O - HCl$-treated tephra leachate (blue unfilled diamonds). Sample codes are listed in Table 1.

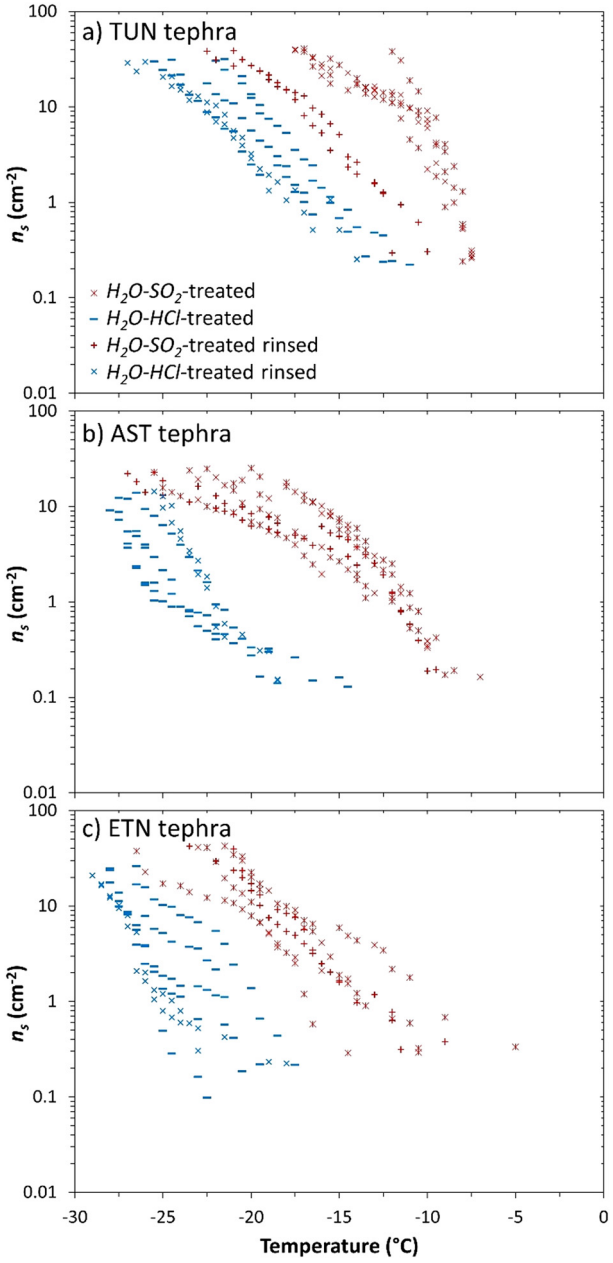

Fig. 6. The effect of rinsing in water on the INA of the $H_2O - SO_2$- and $H_2O - HCl$—treated tephra samples. Ice nucleation active site density (n_s) as a function of temperature for 1 wt.% suspensions of a) TUN tephra, b) AST tephra, and c) ETN tephra in water. These include replicates of the $H_2O - SO_2$-treated (red stars), $H_2O - HCl$-treated (blue dashes), water-rinsed $H_2O - SO_2$-treated (red crosses), and water-rinsed $H_2O - HCl$-treated (blue xs) tephra samples. Sample codes are listed in Table 1.

$CaSO_4$) (Renggli et al., 2019; Ayris et al., 2013), can be seen on the $H_2O - SO_2$-treated AST tephra by scanning electron microscopy - energy dispersive X-ray spectroscopy (SEM-EDX; Fig. 7; see the SI for details). Such deposits are absent on the surface of the non-treated AST tephra.

Dilute solutions of ammonium salts (e.g., $(NH_4)_2SO_4$, NH_4Cl; 10^{-4} to 1 M) have been shown to increase the INA of some silicates including kaolinite, muscovite, biotite, K-feldspar, Na/Ca-feldspar, and quartz relative to their INA in pure water (Whale et al., 2018; Kumar et al., 2018, 2019a). This has been hypothesised to relate to hydrogen bonding of NH_4^+ or NH_3 with -OH groups on the silicate surfaces, in turn promoting hydrogen bonding with H_2O molecules in preferred orientations for ice formation (Kumar et al., 2018, 2019a; Wei et al., 2002; Anim-Danso et al., 2016). To evaluate whether a solute effect could be responsible for modifying the tephra's ability to nucleate ice, supplementary experiments were performed with TUN-, AST-, and ETN tephra; measuring the INA of the non-treated tephra suspended in the $H_2O - SO_2$-treated tephra leachates in addition to those suspended in Milli-Q water (Fig. 5). The similarity in INA of the non-treated tephra suspended in Na/K/Ca/Mg/SO_4^{2-}-rich leachate (10^{-1} to 1 M; Fig. 4c) and in pure water implies that solute ions on their own are unlikely to explain the altered INA of the $H_2O - SO_2$-treated tephra. Moreover, the $H_2O - SO_2$-treated tephra do not bear ammonium salts as reaction products, and so a positive influence of dissolved NH_4^+ or NH_3 on INA is discounted here. Interestingly, the water-rinsed $H_2O - SO_2$-treated tephra recovered after leaching and filtration

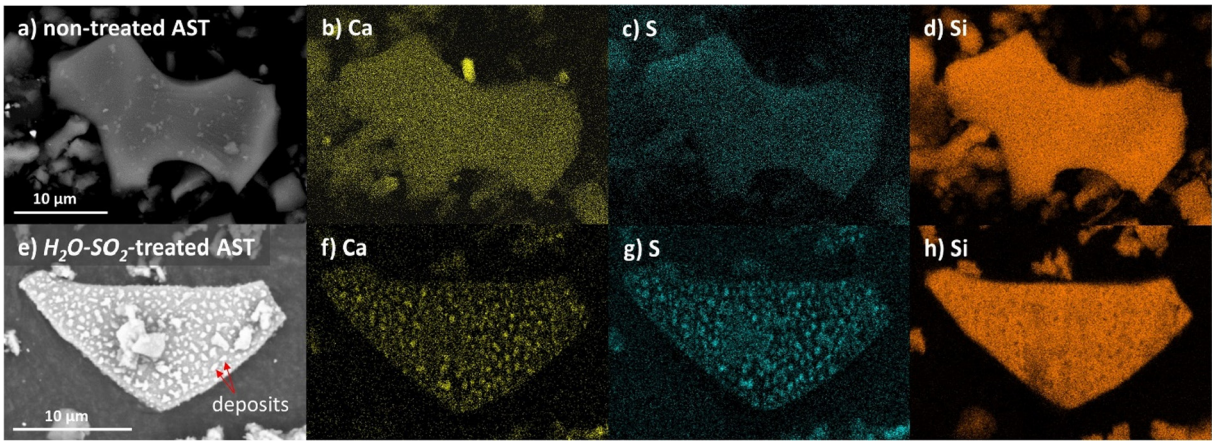

Fig. 7. Back-scattered electron images (Hitachi SU-5000 SEM-EDX) of grains of non-treated (a) and $H_2O - SO_2$-treated (e) AST tephra. The red arrows on the latter point to Ca- and S-rich deposits, likely reflecting $CaSO_4$, formed on the Si-rich tephra surface based on EDX maps of Ca, S, and Si (f-h). Such deposits are absent on the non-treated tephra (b-d).

(see section 2.4) continue to display a higher INA relative to the other treated tephra, although rinsing did reduce the INA of the $H_2O - SO_2$—treated TUN tephra (Fig. 6). Therefore, the $H_2O - SO_2$-treated tephra presumably exhibit some new or altered surface feature that makes them more ice-active than the other treated tephra, despite the likelihood that they all have in common a more oxidised, compact and silica-rich surface layer.

Some surficial $CaSO_4$ was most likely retained on the $H_2O - SO_2$-treated tephra even when immersed in water, as the solubility of this compound (~0.2 g 100 mL^{-1} at 20 °C and 1 atm) is low compared to other alkali and alkaline earth salts (e.g., Na_2SO_4, K_2SO_4, $MgSO_4$, NaCl, KCl, $CaCl_2$ solubilities are ~two orders of magnitude higher; Weast and Lide, 1989) and it might not have dissolved completely on the timescale of the immersion freezing experiments. Therefore, we speculate that surficial $CaSO_4$ contributed to enhancing the INA of the tephra, with this effect partially offset in AST tephra by strong deactivation of its K-feldspar component by the $H_2O - SO_2$ treatment (Table 1, Fig. 2). In order to test the INA of anhydrite, a natural anhydrite specimen from Staffordshire, UK was chosen and found to exhibit a high INA; inducing freezing of water droplets from -4.3 to -10.8 °C (Figure S1 in the SI). There is also strong evidence for coal fly ash that anhydrite, prior to its dissolution in water, promotes ice nucleation at the ash-water interface (Havlíček et al., 1993; Grawe et al., 2018). A correlation has been observed between the amount of Ca- and S-containing compounds and the immersion freezing efficiency of dry-generated coal fly ash samples (Grawe et al., 2018). However, three $H_2O - SO_2$-treated volcanic *glasses* additionally tested here, and which similarly appear to bear surficial $CaSO_4$, do not display a clear increase in INA compared to non-treated glasses (Figure S2 in the SI). This might indicate that the role of $CaSO_4$ in triggering ice nucleation depends on the INA of the original surface, as the non-treated glasses are poorly ice-active to begin with (Figure S2 in the SI) (Maters et al., 2019). Perhaps a combination of differing surface mineralogical and morphological properties of pure glass and mixed glassy/crystalline tephra determines if and how $CaSO_4$ formed on the $H_2O - SO_2$-treated materials acts to influence ice nucleation. Havlíček et al. (1993) suggest that the activity of $CaSO_4$ (and other sulphate salts) in ice nucleation by coal fly ash is affected by the morphology of the ash particles, in particular by the configurations of insoluble and soluble components of the ash surfaces. This conforms to the notion that it is a certain combination of surface chemistry and topography that gives rise to ice-active sites on silicate materials (Harrison et al., 2019; Holden et al., 2019; Whale et al., 2017).

4.4. H_2O-HCl and H_2O-SO_2 depress the INA of K-feldspar and quartz

For K-feldspar, the adverse effects of $H_2O - HCl$ and $H_2O - SO_2$ exposure on INA exceed that of H_2O exposure alone (Figs. 2, 3), revealing that contact with $HCl_{(g)}$ or $SO_{2(g)}$ has some additional negative influence on the ability of this material to nucleate ice. In contrast to the tephra, the K-feldspar shows no substantial difference in dissolved element or ion concentrations in leachates of the $H_2O - HCl$-treated or $H_2O - SO_2$-treated samples and that of the non-treated sample (Fig. 4a, c, d). This suggests that interaction of K-feldspar with $H_2O_{(g)}$ and $HCl_{(g)}$ or $SO_{2(g)}$ at high temperatures did not involve reaction to produce readily soluble compounds (e.g., KCl, NaCl, K_2SO_4, Na_2SO_4) on its surface. In the case of $HCl_{(g)}$, the reason for this is not known and warrants investigation, as we might have expected Na^+ and K^+ in the feldspar to exchange with H^+ and react with Cl^-. In the case of $SO_{2(g)}$, this observation is consistent with thermodynamic modelling by King et al. (2018), which predicted that no sulphate salts formed on K-feldspar exposed to $SO_{2(g)}$ at 600 °C, although the solid-state controls behind this finding are poorly understood and require further research. The modelling predicted instead a significant amount of SiO_2 formed on the treated K-feldspar (10 mol SiO_2:1 mol K-feldspar), which might have acted as a diffusion barrier against cation outfluxing, thereby hindering reaction with surface adsorbed SO_2 (King et al., 2018). As under the H_2O treatment, heating of the K-feldspar during the $H_2O - HCl$ and $H_2O - SO_2$ treatments might have caused a loss of ice-active sites as its surface becomes less crystalline (Swayze, 1907), with this effect perhaps enhanced by the acidic $HCl_{(g)}$ and $SO_{2(g)}$ (King et al., 2018). If so, the development of a more extensive amorphous silica-like surface on K-feldspar under $HCl_{(g)}$ or $SO_{2(g)}$ might underlie the greater depression in INA observed for the $H_2O - HCl$- and $H_2O - SO_2$-treated samples compared to the H_2O-treated sample. Interestingly, Kumar et al. (2019a) noted an inverse correlation between the thickness of the amorphous silica-enriched surface layer on K-feldspar and its INA (defined by the onset freezing temperature) following exposure of this material to the aqueous acid H_2SO_4 (Kumar et al., 2018).

In contrast to the tephra and K-feldspar, exposure of quartz to $HCl_{(g)}$ or $SO_{2(g)}$ appears to have no additional bearing on the ability of this material to nucleate ice compared to when exposed only to $H_2O_{(g)}$ at high temperatures (Figs. 2, 3). Moreover, it appears that some ice-active surface sites on quartz are not affected whatsoever by treatment with $H_2O - SO_2$, i.e., $n_s(T)$ values of the $H_2O - SO_2$-treated quartz are comparable to those of the non-treated quartz at temperatures above ~-15 °C (Fig. 2). The apparent insensitiv-

ity of the INA of quartz to contact with $HCl_{(g)}$ or $SO_{2(g)}$ in addition to $H_2O_{(g)}$ might relate to the lack of exchangeable cations in this material. In contrast to the tephra, the quartz exhibits similar dissolved element and ion concentrations in leachates of the $H_2O - HCl$-treated, $H_2O - SO_2$-treated, and non-treated samples (Fig. 4a, c, d), indicating that quartz interaction with $H_2O_{(g)}$ and $HCl_{(g)}$ or $SO_{2(g)}$ at high temperatures did not involve reaction to produce readily soluble compounds on its surface. The absence of soluble chloride or sulphate salts on quartz exposed to $HCl_{(g)}$ or $SO_{2(g)}$ is not surprising, as this mineral is practically devoid of alkali or alkaline earth cations with which to react. Such metal cations are hypothesised to act as Lewis acid surface sites involved in $HCl_{(g)}$ chemisorption (through the Cl^- end) and to be associated with Lewis base O^{2-} or OH^- surface sites involved in $SO_{2(g)}$ chemisorption on multi-oxide silicates including volcanic ash and glass (Delmelle et al., 2018; Maters et al., 2017). In fact, fused quartz is considered relatively inert and thermally stable, and for these reasons makes up components of the AGAR device and other high temperature reactors (Ayris et al., 2013; Sung et al., 2009; Li et al., 2010; Ayris et al., 2015). Therefore, as under H_2O treatment, the adverse effect of $H_2O - HCl$ and $H_2O - SO_2$ treatments on the INA of the quartz material here is inferred to relate to the creation of a partially dehydroxylated and more compact surface, which bears fewer sites for hydrogen bonding with water and/or taking up protons in aqueous solution.

4.5. Remarks on potential physical effects

In addition to chemical differences between the treated and non-treated silicate materials, the eruption plume processing experiments might have modified physical properties of the solid samples affecting ice nucleation.

The SSA_{BET} (Table 1) is consistently lower for the treated samples than for the non-treated samples, revealing that the gas-solid interactions at high temperatures reduced solid surface area. The treatments may have caused loss of some features associated with surface roughness such as steps, kinks and cracks, as unstable high-energy patches can disappear due to structural relaxation of silicate surfaces at high temperatures under $H_2O_{(g)}$ (Agarwal and Tomozawa, 1997). These high-energy features may also be more susceptible (than flat surfaces) to alteration by $H_2O_{(g)}$ and $SO_{2(g)}$ or $HCl_{(g)}$. Moreover, gas-solid reactions can alter physical properties of particles in various ways, with porosity and permeability for instance being created or destroyed as reaction products modify particle architecture (King et al., 2018). In the case of the tephra treated to $H_2O - SO_2$ and $H_2O - HCl$, the reduction in surface area could partly reflect a masking of internal surface by newly-formed metal sulphates and chlorides, which have a higher molar volume than their corresponding metal oxides (King et al., 2018). Microscopic analysis of silicate glasses treated with $SO_{2(g)}$ at high temperatures reveals $CaSO_4$ deposits of various morphologies (e.g., wrinkled, buckled, hillocked, ringed, rounded) (Renggli et al., 2019; Casas et al., 2019), such deposits are similarly seen here on the AST tephra treated to $H_2O - SO_2$ (Fig. 7). Reaction products might conceivably also increase surface area by introducing additional topography, but this is not evidenced by the SSA_{BET} data. Given that specific combinations of topographical and chemical features are thought to give rise to ice-active surface sites on silicate materials (Harrison et al., 2019; Holden et al., 2019; Whale et al., 2017), changes in surface texture during the eruption plume processing treatments could contribute to the changes in INA observed (Figs. 3, 4).

It is likely that a combination of effects determines the ability of the silicate materials investigated here to nucleate ice, in a manner that is difficult to disentangle given the widely ranging sample physicochemical properties, and the potentially competing influences of various gas-solid interactions on ice-active surface sites. Future research, for example using simple model systems (e.g., soda-lime-silica beads) to further minimise the number of variables being tested at a time, and surface sensitive analytical techniques to elucidate the changes induced by different plume processing treatments at the scale relevant for ice nucleation, will likely be essential to unravel these effects.

5. Conclusions and implications

Here we combined high temperature gas-solid interaction experiments with ice nucleation measurements to investigate the effects of eruption plume processing on the INA of volcanic ash. The INA of all five silicate materials was depressed by exposure to H_2O or $H_2O - HCl$. Conversely, the INA of the tephra was enhanced by exposure to $H_2O - SO_2$, or else depressed to a lesser degree than by exposure to H_2O or $H_2O - HCl$. Any reduction in INA observed following gas-solid interaction is proposed to reflect a loss of ice-active sites on the silicates potentially due to dehydroxylation, oxidation and/or cation extraction, producing a more hydrophobic, compact and/or amorphous silica-like surface. In contrast, the increase in INA observed following tephra interaction with $H_2O - SO_2$ is hypothesised to reflect the creation of ice-active sites potentially relating to $CaSO_4$ formation. We speculate that such sites arise from a particular combination of surface chemical and topographical features accompanying $CaSO_4$ on the tephra, consistent with previous suggestions on the role of $CaSO_4$ in promoting ice nucleation by coal fly ash (Havlíček et al., 1993; Grawe et al., 2018).

While treatments with $H_2O_{(g)}$ and $SO_{2(g)}$ or $HCl_{(g)}$ were performed separately here, eruption plumes contain mixtures of these and other gases (e.g., $CO_{2(g)}$), which might interact in affecting ash surface properties and INA. However, this is not expected to change the conclusion that exposure to $H_2O_{(g)}$ and $SO_{2(g)}$ at high temperatures can enhance the ash INA, since $CaSO_4$ forms even in mixed gas atmospheres, with $SO_{2(g)}$, $HCl_{(g)}$, and $CO_{2(g)}$ apparently not competing for reactive uptake on ash surfaces (Delmelle et al., 2018; Ayris et al., 2014). Water leachates of ash samples whose natural surfaces have been preserved following collection provide evidence that $CaSO_4$ is often a dominant salt found on ash from volcanic eruptions worldwide (Witham et al., 2005). Metal salts including $CaSO_4$ may also form by precipitation following leaching and dissolution of ash surfaces by $H_2O_{(l)}$, $H_2SO_{4(aq)}$, and $HCl_{(aq)}$ at lower temperatures (<190 °C) in the condensation zone of the eruption plume (see Fig. 1) (Óskarsson, 1980; Delmelle et al., 2007). Such ash-condensate interaction could additionally modify ash physicochemical properties and INA in ways not explored here, although the window of opportunity might be limited before the ash is propelled to temperatures at which ice nucleates. How ash properties are further altered in this interval between high temperature processing and ice nucleation is a target for future study. The dynamics between solid, gas, and liquid phases in an eruption plume remain poorly understood, largely due to the danger and difficulty of direct observations within this environment (Delmelle et al., 2018). Laboratory and modelling studies have an important role to play in shedding more light on ash-gas/condensate interactions and their potential impacts (e.g., on ice nucleation, gas scavenging, ash aggregation), both in the vicinity of a volcano and further afield.

The observations in this study suggest that a combination of factors drives the overall INA of ash following transit through the eruption plume. Ash bulk properties such as mineralogy derived from the source magma might affect INA directly (Maters et al., 2019; Jahn et al., 2019), but they also influence the changes in ash surface properties elicited by ash-gas/condensate interactions in the plume (e.g., salt formation) (Delmelle et al., 2007, 2018),

which likely have an overriding effect on the reactivity of airborne ash including its INA (Maters et al., 2016, 2017). For example, the observed reduction in INA of AST tephra following $H_2O - SO_2$ treatment probably reflects deactivation of its K-feldspar, while no such reduction in INA of TUN- and ETN tephra might suggest that the Na/Ca-feldspar and pyroxene in these samples were not deactivated by $H_2O - SO_2$ (Table 1, Fig. 2a-c) (Maters et al., 2019). Bulk mineralogy has similarly been shown to influence the response of dust INA to thermochemical treatment, with illite and kaolinite powders containing K-feldspar being most susceptible to a loss of ice-active sites upon heating with H_2SO_4 vapour (Wex et al., 2014; Augustin-Bauditz et al., 2014). However, on all three tephra tested here, we infer that surficial $CaSO_4$ formed by reaction with $H_2O_{(g)}$ and $SO_{2(g)}$ promoted ice nucleation. Additional thermochemical treatments of a range of minerals found in ash (e.g., Na/Ca-feldspars, pyroxenes, amphiboles, Fe(-Ti) oxides) are recommended to explore more fully this potential interplay of bulk and surface properties in determining the INA of ash emerging from an eruption plume.

Finally, future experimental research applying surface sensitive analytical techniques (e.g., second harmonic and sum frequency generation spectroscopy) (Anim-Danso et al., 2016) will be valuable to reveal the mechanistic relationships between chemical and physical modifications of silicate surfaces and changes in their INA. The impact of eruption plume processing on condensation freezing and deposition ice nucleation on ash is also worth investigating, especially since surficial salts might differentially affect the INA of ash exposed to H_2O-subsaturated versus H_2O-supersaturated regimes (Sullivan et al., 2010a; Wex et al., 2014). This could be important for predicting the potential of airborne ash to nucleate ice under different conditions of temperature and relative humidity encountered in the troposphere or tropopause following an eruption. The INA of ash bearing $CaSO_4$ is likely to be diminished with time immersed in water (e.g., in cloud droplets), as the anhydrite dissolves and/or develops an adsorbed layer of hydrated ions (Grawe et al., 2018). Lastly, transdisciplinary field studies collecting ash particles and complementary volcanic and atmospheric measurements at different distances from the crater could help to improve understanding of how the INA of ash evolves as it disperses away from the eruption plume into the wider atmosphere, where it is susceptible to further physicochemical processing involving low temperature heterogeneous interactions.

CRediT authorship contribution statement

Elena C. Maters: Conceptualization, Formal analysis, Funding acquisition, Investigation, Resources, Visualization, Writing - original draft, Writing - review & editing. **Corrado Cimarelli:** Funding acquisition, Investigation, Resources, Supervision, Visualization, Writing - review & editing. **Ana S. Casas:** Investigation, Resources, Writing - review & editing. **Donald B. Dingwell:** Funding acquisition, Resources, Writing - review & editing. **Benjamin J. Murray:** Funding acquisition, Resources, Supervision, Writing - review & editing.

Declaration of competing interest

The authors declare that they have no known competing financial interests or personal relationships that could have appeared to influence the work reported in this paper.

Data availability

The data associated with this paper is available from the University of Leeds at https://doi.org/10.5518/890.

Acknowledgements

EM was funded by the European Union's Horizon 2020 Research and Innovation Programme under Marie Skłodowska-Curie Actions grant agreement no. 746695 (INoVA), and benefits from a Leverhulme Trust Early Career Fellowship funded jointly by the Isaac Newton Trust. BM acknowledges the European Research Council (648661; MarineIce) and the Natural Environment Research Council (NE/T00648X/1) for funding. CC acknowledges the support of Deutsche Forschungsgemeinschaft project CI 254/2-1. DBD acknowledges the support of European Research Council 2018 ADV Grant 834255 (EAVESDROP). The authors wish to thank Pierre Delmelle for advice on the AGAR experiments, Ulrich Küppers for collecting the tephra samples, William Orsi for enabling access to ultrapure water facilities at LMU, Mark Holden for helpful hints on the INA data, and Alberto Sánchez Marroquín and Grace Porter for valuable input with error and background calculations. We are grateful to Fiona Keay and Stephen Reid for IC and ICP-OES analyses of the water leachates, and to Lesley Neave, Andy Connelly, and Andy Hobson for laboratory assistance.

Appendix A. Supplementary material

Supplementary material related to this article can be found online at https://doi.org/10.1016/j.epsl.2020.116587.

References

Agarwal, A., Tomozawa, M., 1997. Surface and bulk structural relaxation kinetics of silica glass. J. Non-Cryst. Solids 209, 264–272.
Anim-Danso, E., Zhang, Y., Dhinojwala, A., 2016. Surface charge affects the structure of interfacial ice. J. Phys. Chem. C 120, 3741–3748.
Atkinson, J.D., et al., 2013. The importance of feldspar for ice nucleation by mineral dust in mixed-phase clouds. Nature 498, 355–358.
Augustin-Bauditz, S., et al., 2014. The immersion mode ice nucleation behavior of mineral dusts: a comparison of different pure and surface modified dusts. Geophys. Res. Lett. 41, 7375–7382.
Ayris, P.M., et al., 2013. SO_2 sequestration in large volcanic eruptions: high-temperature scavenging by tephra. Geochim. Cosmochim. Acta 110, 58–69.
Ayris, P.M., et al., 2014. HCl uptake by volcanic ash in the high temperature eruption plume: mechanistic insights. Geochim. Cosmochim. Acta 144, 188–201.
Ayris, P.M., et al., 2015. A novel apparatus for the simulation of eruptive gas-rock interactions. Bull. Volcanol. 77, 1–5.
Casas, A.S., et al., 2019. SO_2 scrubbing during percolation through rhyolitic volcanic domes. Geochim. Cosmochim. Acta 257, 150–162.
Connolly, P.J., et al., 2009. Studies of heterogeneous freezing by three different desert dust samples. Atmos. Chem. Phys. 9, 2805–2824.
Cooper, R.F., Fanselow, J.B., Poker, D.B., 1996. The mechanism of oxidation of a basaltic glass: chemical diffusion of network-modifying cations. Geochim. Cosmochim. Acta 60, 3253–3265.
Delmelle, P., Lambert, M., Dufrêne, Y., Gerin, P., Óskarsson, N., 2007. Gas/aerosol-ash interaction in volcanic plumes: new insights from surface analyses of fine ash particles. Earth Planet. Sci. Lett. 259, 159–170.
Delmelle, P., Wadsworth, F.B., Maters, E.C., Ayris, P.M., 2018. High temperature reactions between gases and ash particles in volcanic eruption plumes. Rev. Mineral. Geochem. 84, 285–308.
Douglas, R.W., Isard, J.O., 1949. The action of water and of sulphur dioxide on glass surfaces. J. Soc. Glass Technol. 33, 289–335.
D'Souza, A.S., Pantano, C.G., 2002. Hydroxylation and dehydroxylation behavior of silica glass fracture surfaces. J. Am. Ceram. Soc. 85, 1499–1504.
Durant, A.J., Bonadonna, C., Horwell, C.J., 2010. Atmospheric and environmental impacts of volcanic particulates. Elements 6, 235–240.
Genareau, K., Cloer, S.M., Primm, K., Tolbert, M.A., Woods, T.W., 2018. Compositional and mineralogical effects on ice nucleation activity of volcanic ash. Atmosphere (Basel) 9, 5–7.
Grawe, S., et al., 2018. Coal fly ash: linking immersion freezing behavior and physicochemical particle properties. Atmos. Chem. Phys. 18, 13903–13923.
Harrison, A.D., et al., 2016. Not all feldspar is equal: a survey of ice nucleating properties across the feldspar group of minerals. Atmos. Chem. Phys. Discuss., 1–26.
Harrison, A.D., et al., 2019. The ice-nucleating ability of quartz immersed in water and its atmospheric importance compared to K-feldspar. Atmos. Chem. Phys. Discuss. 19, 11343–11361.
Havlíček, D., Přibil, R., Školoud, O., 1993. The chemical and mineralogical composition of the water-soluble fraction of power-plant ash and its effect on the process of crystallization of water. Atmos. Environ., A Gen. Top. 27, 655–660.

Hobbs, V.P., Fullerton, C.M., Bluhm, G.C., 1971. Ice nucleus storms in Hawaii. Nat. Phys. Sci. 230, 90–91.
Holden, M.A., et al., 2019. High-speed imaging of ice nucleation in water proves the existence of active sites. Sci. Adv. 5, 1–11.
Holdren, G.R., Speyer, P.M., 1985. Reaction rate-surface area relationships during the early stages of weathering-I. Initial observations. Geochim. Cosmochim. Acta 49, 675–681.
Hu, X.L., Michaelides, A., 2007. Ice formation on kaolinite: lattice match or amphoterism? Surf. Sci. 601, 5378–5381.
Jahn, L.G., Fahy, W.D., Williams, D.B., Sullivan, R.C., 2019. Role of feldspar and pyroxene minerals in the ice nucleating ability of three volcanic ashes. ACS Earth Space Chem. 3, 626–636.
King, P.L., et al., 2018. Gas-solid reactions: theory, experiments and case studies relevant to Earth and planetary processes. Rev. Mineral. Geochem. 84, 1–56.
Kiselev, A., et al., 2017. Active sites in heterogeneous ice nucleation-the example of K-rich feldspars. Science 355, 367–371.
Kumar, A., Marcolli, C., Luo, B., Peter, T., 2018. Ice nucleation activity of silicates and aluminosilicates in pure water and aqueous solutions – part 1: the K-feldspar microcline. Atmos. Chem. Phys. 18, 7057–7079.
Kumar, A., Marcolli, C., Peter, T., 2019a. Ice nucleation activity of silicates and aluminosilicates in pure water and aqueous solutions-part 3: aluminosilicates. Atmos. Chem. Phys. 19, 6059–6084.
Kumar, A., Marcolli, C., Peter, T., 2019b. Ice nucleation activity of silicates and aluminosilicates in pure water and aqueous solutions-part 2: quartz and amorphous silica. Atmos. Chem. Phys. 19, 6035–6058.
Langer, G., Garcia, C.J., Mendonca, B.G., Pueschel, R.F., Fullerton, C.M., 1974. Volcanos–a source of ice nuclei? J. Geophys. Res. 79, 873–875.
Li, E.Y., Chareev, D.A., Shilobreeva, S.N., Grichuk, D.V., Tyutyunnik, O.A., 2010. Experimental study of sulfur dioxide interaction with silicates and aluminosilicates at temperatures of 650 and 850 °C. Geochem. Int. 48, 1039–1046.
Maters, E.C., Delmelle, P., Rossi, M.J., Ayris, P.M., Bernard, A., 2016. Controls on the surface chemical reactivity of volcanic ash investigated with probe gases. Earth Planet. Sci. Lett. 450, 254–262.
Maters, E.C., Delmelle, P., Rossi, M.J., Ayris, P.M., 2017. Reactive uptake of sulfur dioxide and ozone on volcanic glass and ash at ambient temperature. J. Geophys. Res., Atmos. 122.
Maters, E.C., et al., 2019. The importance of crystalline phases in ice nucleation by volcanic ash. Atmos. Chem. Phys. 19, 5451–5465.
Nathenson, M., 2017. Revised tephra volumes for Cascade Range volcanoes. J. Volcanol. Geotherm. Res. 341, 42–52.
Óskarsson, N., 1980. The interaction between volcanic gases and tephra: fluorine adhering to tephra of the 1970 hekla eruption. J. Volcanol. Geotherm. Res. 8, 251–266.
Pedevilla, P., Fitzner, M., Michaelides, A., 2017. What makes a good descriptor for heterogeneous ice nucleation on OH-patterned surfaces. Phys. Rev. B 96, 17.
Pelte, S., et al., 2000. Effects of thermal treatment on feldspar sorptive properties: identification of uptake mechanisms. Miner. Eng. 13, 609–622.
Prata, A.T., et al., 2020. Anak Krakatau triggers volcanic freezer in the upper troposphere. Sci. Rep. 10, 1–13.
Renggli, C.J., et al., 2019. An experimental study of SO_2 reactions with silicate glasses and supercooled melts in the system anorthite–diopside–albite at high temperature. Contrib. Mineral. Petrol. 174.
Salam, A., Lesins, G., Lohmann, U., 2008. Laboratory study of heterogeneous ice nucleation in deposition mode of montmorillonite mineral dust particles aged with ammonia, sulfur dioxide, and ozone at polluted atmospheric concentrations. Air Qual. Atmos. Health 1, 135–142.
Schaeffer, H.A., Stengel, M., Mecha, J., 1986. Dealkalization of glass surfaces utilizing HCl gas. J. Non-Cryst. Solids 80, 400–404.
Schill, G.P., Genareau, K., Tolbert, M.A., 2015. Deposition and immersion-mode nucleation of ice by three distinct samples of volcanic ash. Atmos. Chem. Phys. 15, 7523–7536.
Schnell, R.C., Pueschel, R.F., Wellman, D.L., 1982. Ice nucleus characteristics of Mount St. Helens effluents. J. Geophys. Res. 87, 11109–11112.
Seifert, P., et al., 2011. Ice formation in ash-influenced clouds after the eruption of the Eyjafjallajkull volcano in April 2010. J. Geophys. Res., Atmos. 116, 1–14.
Sullivan, R.C., et al., 2010a. Chemical processing does not always impair heterogeneous ice nucleation of mineral dust particles. Geophys. Res. Lett. 37, 1–5.
Sullivan, R.C., et al., 2010b. Irreversible loss of ice nucleation active sites in mineral dust particles caused by sulphuric acid condensation. Atmos. Chem. Phys. 10, 11471–11487.
Sung, H.J., Noda, R., Horio, M., 2009. Coupled recycling of PVC and glass wastes producing chlorine-free fuels and cement feed stock. Environ. Sci. Technol. 43, 47–52.
Swayze, A.J., 1907. Extraction of potassium compounds from feldspar.
Temuujin, J., Okada, K., MacKenzie, K.J.D., Jadambaa, T., 1999. The effect of water vapour atmospheres on the thermal transformation of kaolinite investigated by XRD, FTIR and solid state MAS NMR. J. Eur. Ceram. Soc. 19, 105–112.
Vali, G., 2019. Revisiting the differential freezing nucleus spectra derived from drop-freezing experiments: methods of calculation, applications, and confidence limits. Atmos. Meas. Tech. 12, 1219–1231.
Van Eaton, A.R., et al., 2015. Hail formation triggers rapid ash aggregation in volcanic plumes. Nat. Commun. 6, 1–7.
Weast, R.C., Lide, D.R., 1989. Handbook of Chemistry and Physics, 70th edition. CRC Press.
Wei, X., Miranda, P.B., Zhang, C., Shen, Y.R., 2002. Sum-frequency spectroscopic studies of ice interfaces. Phys. Rev. B, Condens. Matter Mater. Phys. 66, 854011.
Wex, H., et al., 2014. Kaolinite particles as ice nuclei: learning from the use of different kaolinite samples and different coatings. Atmos. Chem. Phys. 14, 5529–5546.
Whale, T.F., et al., 2015. A technique for quantifying heterogeneous ice nucleation in microlitre supercooled water droplets. Atmos. Meas. Tech. 8, 2437–2447.
Whale, T.F., et al., 2017. The role of phase separation and related topography in the exceptional ice-nucleating ability of alkali feldspars. Phys. Chem. Chem. Phys. 19, 31186–31193.
Whale, T.F., Holden, M.A., Wilson, T.W., O'Sullivan, D., Murray, B.J., 2018. The enhancement and suppression of immersion mode heterogeneous ice-nucleation by solutes. Chem. Sci. 9, 4142–4151.
Witham, C.S., Oppenheimer, C., Horwell, C.J., 2005. Volcanic ash-leachates: a review and recommendations for sampling methods. J. Volcanol. Geotherm. Res. 141, 299–326.
Wu, T., Kohlstedt, D.L., 1988. Rutherford backscattering spectroscopy study of the kinetics of oxidation of $(Mg, Fe)_2SiO_4$. J. Am. Ceram. Soc. 71, 540–545.